The paper was published in the proceedings of XVI Pan-American Conference on Soil Mechanics and Geotechnical Engineering (XVI PCSMGE) and was edited by Dr. Norma Patricia López Acosta, Eduardo Martínez Hernández and Alejandra L. Espinosa Santiago. The conference was held in Cancun, Mexico, on November 17-20, 2019.

Geotechnical Engineering in the XXI Century: Lessons learned and future challenges
N.P. López-Acosta et al. (Eds.)

doi:10.3233/STAL190091

Using DEM to Study the Behavior of Granular Soils Under Cyclic Shear Loading

L. MANJARREZ[a,1] and L. ZHANG[b]
[a] *PhD candidate, Dept. of Civil and Architectural Engineering and Mechanics, University of Arizona, Tucson, AZ 85721.*
[b] *Delbert R. Lewis Distinguished Professor, Dept. of Civil Engineering and Engineering Mechanics, Univ. of Arizona, Tucson, AZ 85721*

Abstract. In this study DEM simulations were performed to analyze the liquefaction of granular soils. Three different simulations were carried out: triaxial test (TX), static direct simple shear test (SDSS) and cyclic direct simple shear test (CDSS). The soil selected for the analysis was Monterey #0/30 sand, its calibration was done in the TX by inhibiting particle rotation during the loading phase. After that, the calibrated set of micro-parameters were tested in the SDSS to observe its response in a different test configuration showing good agreement. Subsequently, the material was subjected to strain-controlled cyclic loading simulating the CDSS. In the CDSS, the excess pore pressure was measured following the constant-volume approach in loose, medium and dense samples. Overall, the numerical simulations agreed well with the experimental results.

Keywords. Liquefaction, discrete element method, PFC3D, cyclic loading.

1. Introduction

The characterization of saturated soils under seismic loading conditions is of great iterest when designing against earthquakes. The direct simple shear test (DSS) has been widely used for soil characterization since the field stress conditions that involve the rotation of principal stresses are simulated more realistically as [1].

The rapid computational development has allowed to simulate laboratory tests more efficiently. The Discrete Element Method (DEM) has been used as a popular tool to simulate the behavior of soils at a micro-scale level [1–6]. The Particle Flow Code (PFC), which is based on DEM, has been used to study the behavior of saturated soils under cyclic loading conditions in 2D (PFC2D) and 3D (PFC3D).

In DEM, the change in pore pressure is commonly measured in two ways: by assuming no change in volume during the loading phase (constant-volume approach) and by coupling the interaction between the particle and the fluid. The latter is more sophisticated due to the use of advanced programming, while the former is simpler and is based on several assumptions as discussed later.

Several authors have studied the behavior of saturated granular soils in PFC. For example, Yang et al. [7] investigated the liquefaction of saturated stratified silty sands in PFC2D. The results demonstrated that the distribution of normal contacts and contact

[1] Corresponding Author, E-mail: linofmm@gmail.arizona.edu

forces between the particles were affected by the load excitation indicating the onset of liquefaction. Dabeet et al. [4, 8] investigated the liquefaction of granular samples in PFC3D. The constant volume approach was followed to obtain the pore pressure increments by measuring the decrease of the vertical stress. The results were in agreement with the cyclic direct simple shear test (CDSS) laboratory results of specimens containing glass beads. The authors concluded that the DEM simulations captured well the cyclic shear behavior, including pore water pressure measurements.

In this study, DEM simulations are compared with the experimental results from three laboratory studies on Monterey #0/30 sand [9–11]. First, the calibration of the sand was obtained based on Lade [9] where drained triaxial tests were performed under various stress confinement levels at the same relative density. Second, the calibrated material was subjected to static simple shear tests under different normal stress levels and its response was compared with the experimental results presented by Kwan and El Mohtar [11]. Finally, strain-controlled cyclic direct simple shear tests were carried out in the calibrated material following the results of Hazirbaba and Rathje [10] and the constant-volume approach to evaluate the change in excess pore pressure and the reach of liquefaction.

2. Experimental studies description

Monterey #0/30 sand is a medium sized, uniform and clean, quartz beach sand which grain shapes go from sub-angular to sub-rounded [12,13]. Gallagher and Mitchell [14] pointed out that Monterey #0/30 sand gradation curve is located within the curves threshold of most liquefiable soils. A typical grain size distribution curve is shown in Figure 1. Its properties are summarized in Table 1.

Table 1. Monterey #0/30 properties [15].

D_{50} (mm)	C_c	C_u	G_s	e_{min}	e_{max}	$\gamma_{d,\,min}$ (kN/m^3)	$\gamma_{d,\,max}$ (kN/m^3)
0.35	1.29	0.28	2.64	0.541	0.885	13.96	16.81

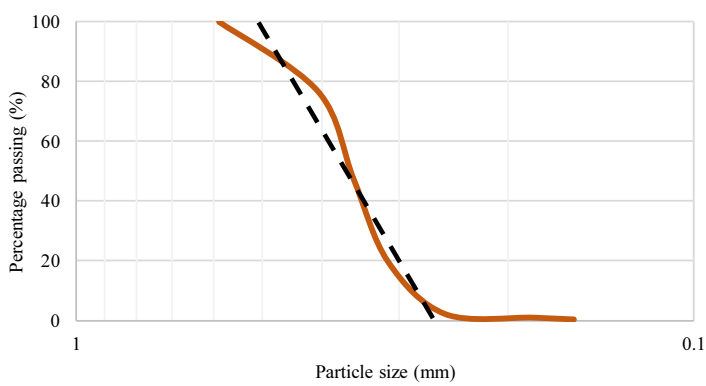

Figure 1. Grain size distribution curve of Monterey #0/30 sand (modified from [15]).

2.1. Drained Triaxial Test

Lade [9] conducted drained triaxial tests at three confining pressures of 0.3, 0.6 and 1.2 MPa. The specimens were compacted at initial void ratios of 0.786, 0.783 and 0.781.

2.2. Static direct simple shear test

Kwan and El Mohtar [11] conducted static direct simple shear test (SDSS). The specimens were consolidated at vertical normal stresses of 25, 50, 75 and 100 kPa before shearing. While in shearing, the consolidation stress was constant in the vertical direction. Loose samples with a relative density range from 28%-44% were tested (equivalent porosity range 0.436-0.421). The experiment was stopped at 25% of shear strain (γ).

2.3. Cyclic simple shear test

Hazirbaba and Rathje [10] conducted strain-controlled cyclic direct simple shear tests (CDSS) on Monterey #0/30 sand to investigate the liquefaction on loose, medium and dense sand specimens. The specimens were compacted in a NGI-type specimen. A normal stress (σ_N) of 100 kPa was used to consolidate the specimens. Liquefaction was reached when the excess of pore pressure ratio (ratio of the recorded excess pore water pressure to the initial vertical effective stress, $u_e=\Delta u/\sigma v'$) was above 90%. All tests were stopped after 50 cycles of loading or when liquefaction was reached, whichever occurred first.

The experimental results were carried out under three different sample densities and three levels of shear strain. Loose, medium and dense samples corresponding to relative densities of 32%, 50% and 93%, respectively. Different levels of strains were tested on each relative density, a summary of the results is presented in Table 2 and the results corresponding to loose samples are shown in Figure 4.

Table 2. Summary of cyclic study results by [10].

Sample density	Shear strain (%)	Excess pore pressure after 1st cycle (%)	Excess pore pressure after 50th cycles (%)	Cycles to reach liquefaction
Loose	0.03	3	34	-
	0.10	10	62	-
	0.30	21	90	20
Medium	0.35	2	19	-
	0.10	7	52	-
	0.30	18	90	30
Dense	0.03	1	11	-
	0.10	7	31	-
	0.30	21	89	-

3. DEM model description

In the DEM, simple stress-strain laws are implemented to study the soil as a discontinuum medium. To model sand behavior, the properties shall be calibrated through DEM micro-parameters, the calibration was performed in a triaxial test set up.

3.1. Particle size and specimen dimensions

The particle size is the first selected micro-parameter. A line was drawn over the grain size distribution curve to match all the possible grain sizes (dashed line in Figure 1). A minimum particle diameter (D_{min}) of 0.25 mm and a maximum to minimum diameter (D_{max}/D_{min}) ratio of 2.0 were defined. All the particles in the model were spheres with a uniform size distribution, and the interaction between particle-particle and particle-wall was governed by the soft contacts approach to represent a cohesionless material [16].

The triaxial specimen dimensions are 9.375 mm diameter and 18.750 mm height. The material was enclosed by two horizontal plane walls and a cylinder wall. An initial porosity (n) of 0.439 was used and around 30,000 particles were generated.

Since all simulations were performed under very low wall velocity, viscous damping had a small effect on the results. A viscous damping of 0.7 was selected since no significant differences were observed when this value was different. The time step was set to $2e^{-5}$ s to reduce the computational time.

3.2. Effect in particle rotation

The simulation of granular interlocking was perfomed by inhibiting particle rotation during the loading phase [17–19]. An important modification from [18] was made since the particle rotation was prevented only in a certain number of particles.

The selection of the coefficient of friction (μ) was closely related to the percentage of particles to be fixed. A μ = 0.475 and 50% of particles fixed were selected since the stress-strain behavior at a confining stress of 1.2 MPa was similar than the reported by [9].

3.3. Static direct simple shear (SDSS)

In the simulations the particles were created inside a specimen with D = 15 mm and H = 3.75 mm. The NGI-type specimen consisted of two horizontal walls, top and bottom (XZ plane), and 14 lateral rings (walls).

Loose samples were formed at n = 0.427 and around 15,000 particles were created.

3.4. Cyclic direct simple shear (CDSS)

In the CDSS simulations, specimen characteristics are the same as the SDSS simulations. A change in the load application was made in CDSS by assigning strain-controlled cyclic loading to each lateral ring by means of a cosine function. The cosine function is given by:

$$cyclic\ loading = A\cos(2\pi f * time) \tag{1}$$

where A, is the amplitude and defines the loading magnitude and f, is the frequency at which the load is applied ($f = 2\ Hz$). The same principle used in SDSS regarding to lateral ring loading was followed, the top lateral ring received the largest loading and it decreased linearly downwards by reducing the amplitude. The loading magnitude controls the lateral ring displacement in positive and negative x directions (Figure 2).

The pore pressure measurements were inferred by following the constant-volume approach. This approach was achieved during cyclic shearing by fixing the top and bottom walls of the specimen in the vertical direction, so no volume change occurs. Finn et al. [20] and Dyvik et al. [21] proved that when no pore pressure measurements are available in CDSS tests, granular soil can be tested in dry conditions and pore pressure measurements can be inferred by the decrease (or increase) of normal stress (normal effective stress, σ_v'). This change would be equivalent to the increase (or decrease) of excess pore pressure in a real undrained test.

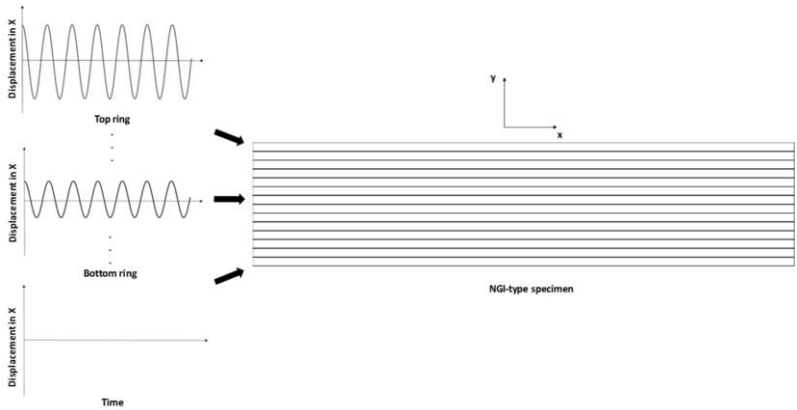

Figure 2. 2D scheme of cyclic load application.

Loose, medium and dense sand specimens were tested at 0.30%, 0.10% and 0.03% of shear strain as presented in [10]. All samples were consolidated at a normal stress of 100 kPa, in this case $\sigma_N = \sigma_v' = 100$ kPa. Simulations were stopped at a $u_e = 95\%$ or after 50 loading cycles (N_{cyc}), whatever occurs first.

The porosities that represent the experimental results are 0.427, 0.420 and 0.411 for loose, medium and dense specimens, respectively.

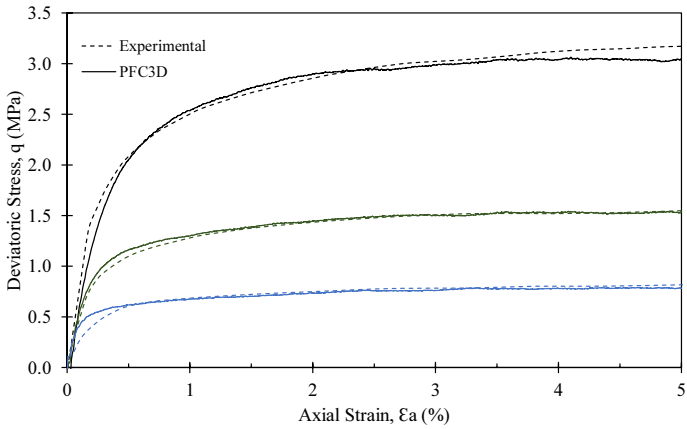

Figure 3. Drained triaxial tests results of calibrated Monterey sand at three different confinement stresses: 1.2, 0.6 and 0.3 MPa.

4. Results of numerical simulations

Figure 3 shows the results reported by [9] and the numerical simulation results. Table 3 summarizes the micro-parameters used in the simulations. After calibration, the material was tested on SDSS and strain-controlled CDSS.

Table 3. Calibrated micro-parameters to represent Monterey #0/30 sand.

Particle properties		Particle dimension		Specimen dimension	
Particle density, ρ (kg/m^3)	2500	Minimum particle radius, Rmin (mm)	0.125	Ratio of minimum specimen length to average particle diameter, L/d_{50}	25
Young's modulus, Ec (GPa)	2.0	Maximum to Minimum particle radius ratio, Rmax/Rmin	2.0	Minimum length (diameter), L = D (mm)	9.375
Coefficient of friction, μ	0.475	Average particle diameter, d_{50} (mm)	0.375	Height (mm)	18.75
Normal to shear stiffness ratio, kn/ks	1.0	Total number of particles	29904		

4.1. Static direct simple shear (SDSS)

The objective of testing the calibrated material in a SDSS is to observe its performance when subjected to different specimen dimensions and loading conditions. For the SDSS, the particle properties and particle dimensions presented in table 3 remained constant. The results were compared with static direct simple shear lab results presented in [11].

Figure 4 shows the simulation results of the SDSS. Some variations are observed, however, the results represent well the experimental SDSS of Monterey #0/30 sand.

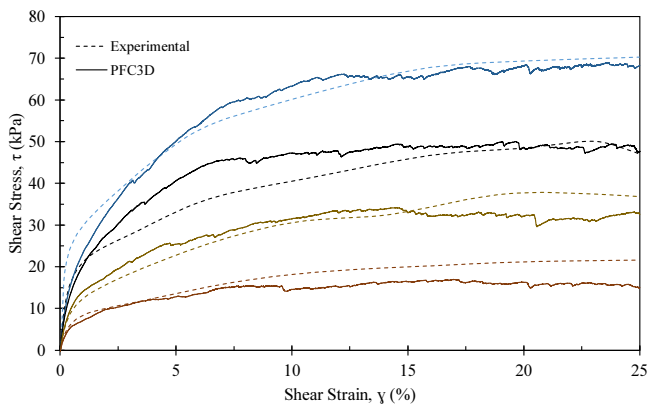

Figure 4. Simulation results of SDSS compared against experimental results.

4.2. Cyclic direct simple shear (CDSS)

Figure 5 shows the simulation results of the loose specimen. The initial assembly was formed by 15019 particles, after consolidation and before the cyclic loading phase, 1270 particles picked at random locations were deleted to reach the desired porosity. Corresponding to the simulation at γ = 0.30%, after the first cycle of loading u_e = 27%,

and a difference of about 6% was observed with the experimental results. Also, the numerical sample reaches u_e = 90% (condition followed by experimental tests) at N_{cyc}=16; it took 4 cycles less to reach liquefaction compared to experimental results. Related to the simulation with γ=0.10%, a slightly overestimation of u_e is observed after N_{cyc}>16, however, it generally shows a good match with experimental results. A similar overestimation of u_e is observed at γ = 0.03% after N_{cyc} > 4, but the overall plot trend agrees with the experimental plot. The results for medium and dense specimens are summarized in Table 4.

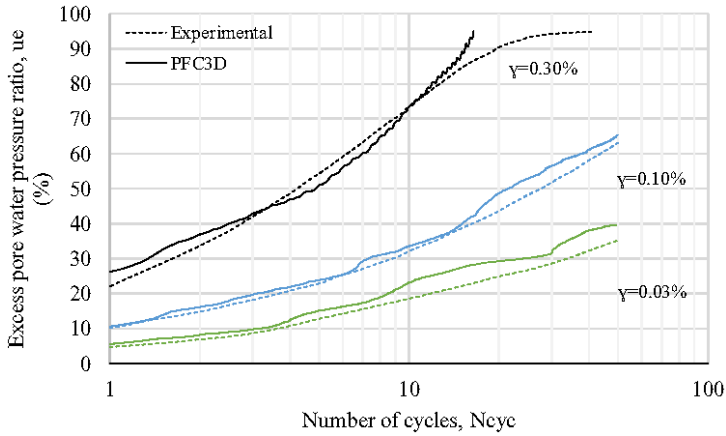

Figure 5. Excess pore water pressure generation in loose Monterey #0/30 sand samples.

Table 4. Summary of simulation results.

Density	γ (%)	u_e after 1st cycle (%)		u_e after 50 cycles (%)		N_{cyc} to liquefy	
		Experimental	This study	Experimental	This study	Experimental	This study
Loose	0.03	3	5	34	40	-	-
	0.10	10	10	62	65	-	-
	0.30	21	27	90	90	20	16
Medium	0.03	2	2	19	15	-	-
	0.10	7	7	52	61	-	-
	0.30	18	24	90	90	30	24
Dense	0.03	2	2	10	11	-	-
	0.10	7	7	31	44	-	-
	0.30	21	21	89	90	-	40

In Figure 6 typical plots of strain-controlled CDSS tests are presented (due to space limitations only plots of dense specimens are presented). Figures. 6a, 6c and 6e show the shear strain vs shear stress plot, it is noted that larger shear stresses are developed when γ is larger. In Figure 6a it is seen that the shear stress decreases to a close to zero value. This behavior is not observed in 6c and 6e due to those specimens did not reach liquefaction. In Figures. 6b, 6d and 6f the effective stress vs shear stress plots are shown. In Figure 6b is noted that σ_v' decreases with loading cycles until σ_v' is close to zero. In Figures. 6d and 6f the σ_v' decreased up to 52 kPa and 79 kPa, respectively.

5. Conclusions

In this study, the capabilities of DEM to estimate the excess pore pressure increase on saturated sand specimens subjected to cyclic loading has been demonstrated. Three different laboratory tests were simulated in PFC3D (triaxial, direct simple shear and cyclic direct simple shear) and then compared with laboratory experiments on Monterey #0/30 sand. The inhibition of particle rotation on the loading phase played a key role in the material calibration since it roughly simulated the particle interlocking of soils. The excess pore pressure increase was measured by following the constant-volume approach in the cyclic tests. Overall, the numerical simulations agreed well with the experimental results.

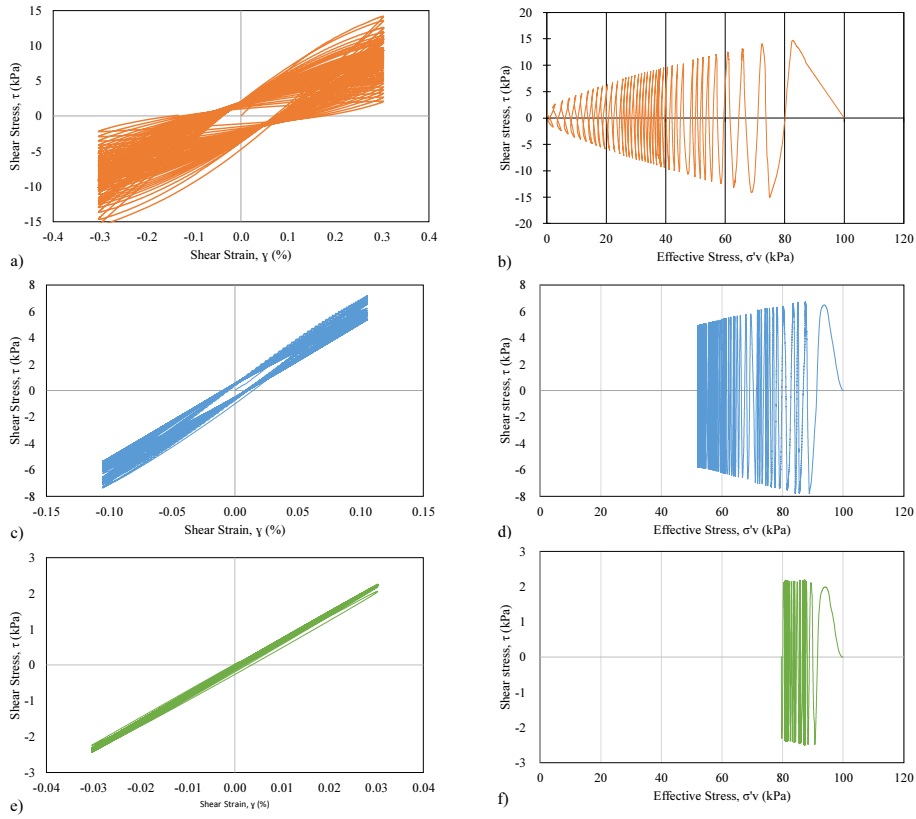

Figure 6. Simulation results of dense sample at three different shear strains: a) γ=0.30%, b) γ=0.10% and c) γ=0.03%.

References

[1] A.K. Ashmawy, B. Sukumaran, V. V Hoang, Evaluating the Influence of Particle Shape on Liquefaction Behavior Using Discrete Element Modeling, in: PCW, 2003: pp. 1–8.

[2] C. O'Sullivan, L. Cui, O'Neill, Discrete element analysis of the response of granular materials during cyclic loading, Soils Found. 48 (2008) 511–530.

[3] S. Anitha, T. Sitharam, Effect of Particle Shape on the Cyclic Stress-Strain Behaviour of Granular Media, in: Indian Geotech. Conf., 2010.
[4] A. Dabeet, D. Wijewickreme, P. Byrne, Simulation of Cyclic Direct Simple Shear Loading Response of Soils Using Discrete Element Modeling, in: 15 WCEE Lisboa, 2012.
[5] J. Jung, J.C. Santamarina, K. Soga, Stress-strain response of hydrate-bearing sands : Numerical study using discrete element method simulations, J. Geophys. Res. 117 (2012) 1–12. doi:10.1029/2011JB009040.
[6] C.J. Coetzee, E. Horn, Calibration of the Discrete Element Method Using a Large Shear Box, Int. J. Mech. Aerospace, Ind. Mechatron. Manuf. Eng. 8 (2014) 2134–2143.
[7] Y. Yang, J. Hu, J. Wang, Numerical Simulation of Meso-mechanism of Liquefaction in Saturated Stratified Silty Sands, Adv. Mater. Res. 601 (2013) 222–226. doi:10.4028/www.scientific.net/AMR.601.222.
[8] A. Dabeet, D. Wijewickreme, P. Byrne, Discrete element modeling of direct simple shear response of granular soils and model validation using laboratory element tests, in: Geotech. Congerence, 2011.
[9] P.V. Lade, The stress-strain and strength chracteristics of cohesionless soils, University of California, Berkeley, 1972.
[10] K. Hazirbaba, E.M. Rathje, Strain-based pore water pressure generation in clean sands, in: Proc. 8th U.S. Natl. Conf. Earthq. Eng. April 18-22, 2006, San Fr. California, USA, 2006.
[11] W.S. Kwan, C. El Mohtar, Comparison between Shear Strength of Dry Sand Measured in CSS Device using Wire-reinforced Membranes and Stacked Rings, in: GeoCongress 2014 Geo-Characterization Model. Sustain., Atlanta, GA, 2014.
[12] W.A. Charlie, M.W. Muzzy, D.A. Tiedemann, D.O.D. I, R. Charlie, Cyclic Triaxial Behavior of Monterey Number 0 and Number 0 / 30 Sands, Geotech. Test. J. 7 (1984) 211–215.
[13] J. Wu, Liquefaction triggering and post-liquefaction deformation of Monterey 0/30 sand under uni-directional cyclic simple shear loading, 2002.
[14] P.M. Gallagher, J.K. Mitchell, Influence of colloidal silica grout on liquefaction potential and cyclic undrained behavior of loose sand, Soil Dyn. Earthq. Eng. 22 (2002) 1017–1026.
[15] A.M. Kammerer, J.M. Pestana, R.B. Seed, Undrained Response of Monterey 0 / 30 Sand Under Multidirectional Cyclic Simple Shear Loading Conditions, University of California, Berkeley, 2002.
[16] Itasca Consulting Group, PFC3D manual, version 4.0, Minneapolis, 2008.
[17] F. Calvetti, Discrete modelling of granular materials and geotechnical problems Discrete modelling of granular materials and geotechnical problems, Eur. J. Environ. Civ. Eng. 12 (2008) 951–965. doi:10.3166/EJECE.12.951-965.
[18] M. Arroyo, J. Butlanska, A. Gens, F. Calvetti, M. Jamiolkowski, Cone penetration tests in a virtual calibration chamber, Geotechnique. 61 (2011) 525–531. doi:10.1680/geot.9.P.067.
[19] J. Butlanska, Cone penetration test in a virtual calibration chamber, Universitat Politecnica De Catalunya, 2014.
[20] W.D.L. Finn, Y.P. Vaid, S.K. Bhatia, Constant volume simple shear testing, in: Second Int. Conf. Microzonat. Safer Constr. Appl., San Francisco, California, 1978: pp. 839–851.
[21] R. Dyvik, T. Berre, S. Lacasse, B. Raadim, Comparison of truly undrained and constant volume direct simple shear tests, Geotechnique. 37 (1987) 3–10.